Photon Assay: A New, Revolutionary Technique Everybody Wants to See Succeed – An Independent Evaluation Part 2: The Effect of Positional Heterogeneity on Gold Determinations Using PhotonAssay

By Robert Oliver[1] and Dominique François-Bongarçon

DOI: 10.62178/sst.005.005

ABSTRACT

PhotonAssay™ employs gamma activation analysis to provide rapid, non-destructive determination of gold in large (typically 400–650 g) samples. While the larger sample sizes are presumed to offer significant advantages for heterogeneous, coarse-gold bearing materials compared with traditional fire assay, the reported gold grades may be influenced by uneven spatial distribution of gold particles within the jar. This study investigates the effect of positional heterogeneity i.e. the uneven weighting of different regions within the PhotonAssay jar, on gold determinations.

Low- and medium-resolution maps of instrument response were generated by placing single, accurately weighed gold fragments at precisely controlled locations within filled jars and performing multiple replicate assays. Results reveal differences in weighting: the geometric center of the jar receives the highest response, while regions near the sides and, to a lesser extent, the top and bottom are under-weighted. These findings are consistent with non-uniform irradiation as the dominant source of the observed biases, with gamma-ray attenuation and detection geometry appearing less influential.

The positional weighting introduces a previously under-appreciated source of grouping and segregation error, even after the final assay charge has been prepared. This has important implications for assaying coarse-gold ores, where dense gold particles can segregate during handling and jar filling. The results suggest that PhotonAssay protocols may be vulnerable to biases in certain coarse-gold systems.

1. Background

PhotonAssay is a proprietary process owned by Chrysos Corporation for the determination of gold, silver and copper content in a diverse range of materials. This work focuses on PhotonAssay gold determinations using the standard gold service PAAU02, which are carried out by gamma activation analysis (GAA). A sample of the material to be analyzed is placed into a specialized, roughly cylindrical, high-density polyethylene jar. The jar is capped and weighed. The proportion of the jar's volume occupied by the sample is estimated by fill-o-meter, and the jar is handed off to a robotic system.

The jar is paired with a metal disc containing a reference element, and a linear accelerator (linac) generated 8.5 MeV photon beam is directed at the jar while it is rotated around its axis of circular symmetry.

Gold found naturally in the earth's crust is mono-isotopic, consisting exclusively of 197Au. When irradiated with sufficiently energetic photons, 197Au may become excited and enter a local energy minimum known as a metastable nuclear isomer (equation 1).

$$^{197}Au \xrightarrow{\gamma} {}^{197m}Au \quad (1)$$

1 Director of Laboratory & Technical Operations at ElementUSA

After irradiation, the jar is moved to a measurement chamber with two high-purity germanium detectors arranged above and below the sample. The metastable nuclear isomer 197mAu has a half-life of 7.76 s and undergoes radioactive decay back to the ground state with the emission of a 279 KeV gamma ray [1] (equation 2).

$$^{197\,m}Au \rightarrow {}^{197}Au + \gamma \qquad (2)$$

The count of gamma emissions detected by the HPGe detectors at 279 KeV will be proportional to the amount of gold present in the sample. For the standard gold service PAAU02, this process is repeated twice for each jar, with 15 seconds of irradiation time and 15 seconds of measurement time per cycle [2]. Chrysos Corporation states that the process provides true bulk analysis of 400 – 650 g samples [3]. An assay charge of this size is more representative of the bulk material than a conventional fire assay charge (typically up to 50 g). This has distinct advantages when assaying ores containing coarse gold particles [4].

The exact process through which the 279 keV signal is used to determine the gold grade is a trade secret, however relevant factors include: time elapsed since irradiation, mass of sample, occupied jar volume, linac power, reference signals, interfering signals, and, critically for this work, spatial distribution of gold within the jar relative to the excitation beam and detectors, among others. Previous work by Dominy, et al [5] investigated the effect of reorganizing the position of gold-containing fragments within a PhotonAssay jar on the instrument's reported gold grade. Samples of coarse-gold-bearing ore were placed in PhotonAssay jars, assayed, then subsequently shaken for 30 seconds and re-assayed. This procedure was found to induce an insignificant negative bias and negligible increase in total measurement error.

The authors dubbed the uneven distribution of gold throughout a sample positional heterogeneity (similar to distribution heterogeneity as described by Gy).

The process of shaking a jar containing a coarse-gold ore may have two outcomes. Firstly, it may induce segregation of gold fragments within the jar, leading to a tendency for shaken jars to have a greater concentration of gold fragments in particular regions of the jar. On the other hand, shaking the jar may induce no meaningful gold fragment segregation, and simply randomly rearrange their locations.

While in the case investigated by Dominy, et al., only insignificant bias was noted, the presence of an increase in total measurement error, even a negligible one, indicates unequal weighting of different jar regions in grade determination. The absence of significant bias after shaking tends to indicate that the shaking procedure does not induce net segregation of gold fragments between regions of high and low weighting. No detail was given on the mode of shaking, limiting the ability to draw inferences on expected segregation tendencies.

The location of a gold fragment within a jar may impact both its irradiation by the excitation beam, and the detection of decay emissions. The rotation of the jar during irradiation should limit preferential activation of gold fragments on any side or along any diameters (Figure 1).

A beam centered on the jar with a width less than the jar could lead to preferential activation of gold fragments near the center of the rotational axis. The same could be true for a beam with non-uniform intensity across its width. As the beam centering, width and consistency are not known, this simply represents one possible example of how unequal weighting of jar regions can occur.

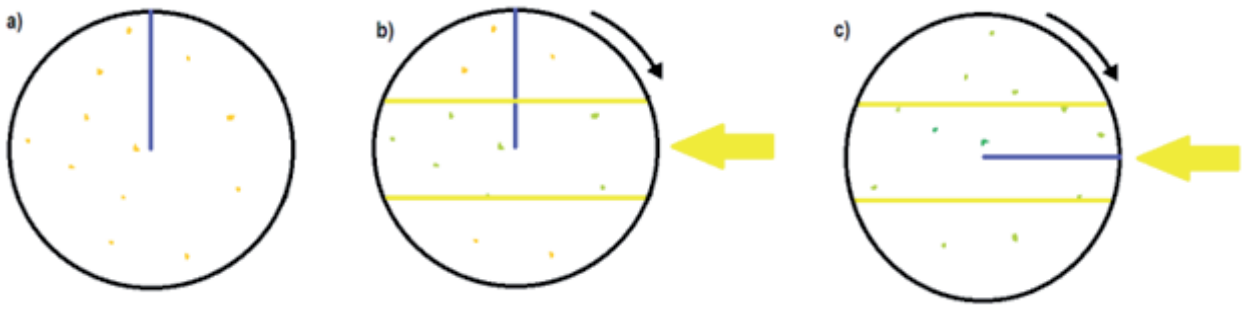

Figure 1: Top down view of PhotonAssay jar; a) depicts jar prior to irradiation with unactivated gold fragments in orange and with blue reference line indicating rotation; b) depicts jar at beginning of irradiation, excitation beam direction and edges in yellow, with activated gold fragments in light green and black arrow indicating direction of rotation; c) depicts jar once all gold fragments have been activated, fragments with longer periods within the beam path in dark green.

Similarly, the detection of gamma emissions originating in some jar regions may be more likely than those from others. The amount of gamma attenuating mass in the emission's path, as well as proportion of possible paths that intersect a detector may affect its weighting in the gold grade determination.

The aim of the present work is to determine the relative weighting of the regions of the jar.

2. Experimental

Two sets of experiments were conducted to produce low-resolution, medium-resolution maps of the detector response to gold particles throughout the jar's volume. While the medium-resolution map is more detailed and the locations more precisely defined, the technique used to construct the low-resolution map enabled particles to be placed at more extreme points in the jar, far from the geometric center.

2.1 Low-resolution Jar Map

A lot of approximately 1000 kg of nominal ¼ inch fragment size rock was obtained from Rail City Garden Center in Reno, Nevada. Riffle splits were taken for preparation and 30 g fire assay to verify gold content was less than 0.005 mg/kg. Approximately 1 kg of material was split from the lot and crushed to 100% passing a 2 mm screen. The crushed material was repeatedly riffle split to completely fill a PhotonAssay jar. Gold powder of purity ≥99.99% and fragment size <850 µm was obtained from Sigma Aldrich and a fragment was separated and accurately weighed.

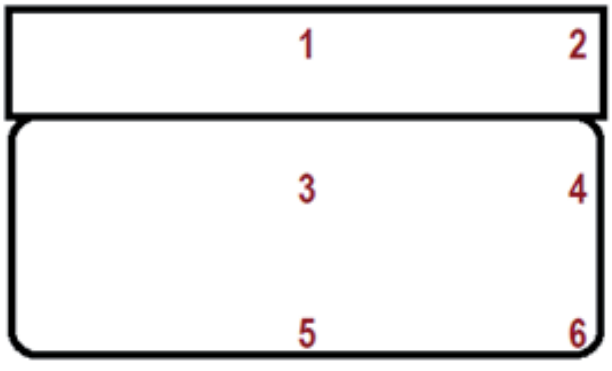

Figure 2: Cross-section of a PhotonAssay jar with the gold fragment locations indicated.

The fragment was immobilized on a piece of scotch tape and affixed to a specific location within the filled jar. With the fragment in that location, the jar was submitted to the PhotonAssay process ten times. The fragment was then moved to another location for ten assays.

This was repeated for six different locations within the jar (Figure 2).

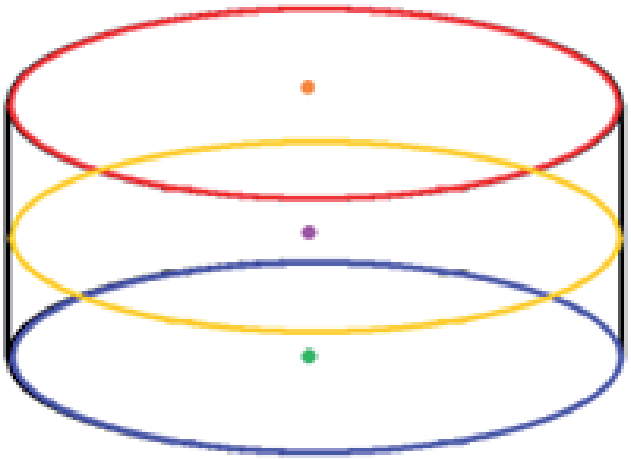

Figure 3: 3D wire-frame projection of jar with location 1 indicated by an orange point, 3 by a purple point, 5 by a green point, 2 by a red circle, 4 by a yellow circle and 6 by a blue circle.

Locations 1, 3 & 5 are points at the center top, center middle, and center bottom of the jar respectively. Due to the random rotational orientation of the jar when irradiation begins, a fragment at location 2, 4 or 6 may start at any point along a circle in a plane perpendicular to the jar's axis of circular symmetry. As a result, locations 2, 4 and 6 are not points but circles at top, middle and bottom respectively (Figure 3).

The material rejected in the splitting operation was pulverized to 85% passing a 75 µm screen. The pulverized material was repeatedly riffle split to completely fill a second PhotonAssay jar. This jar was then likewise subject to PhotonAssay ten times for each gold fragment location using a separately weighed gold fragment.

2.2 Medium-resolution Jar Map

2.2.1 Gold Fragment Positioning Rig

A PhotonAssay jar was taken and filled with epoxy resin which was allowed to solidify. The jar was mounted in a precision lathe and adjusted to a runout of <1 mm. A 12.7 mm hole was drilled into the center of the epoxy resin and end-milled to a flat bottom stopped just as contact was made with the HDPE jar.

The jar was then removed from the lathe and mounted in the compound table of a drill press. Additional 12.7 mm holes were drilled and end-milled to a flat bottom of the same depth as the center hole at 14 mm, 28 mm and 32 mm from the center.

2.2.2 Gold Fragment Positioning Rod

Separately, nylon bar stock was turned down to approximately 12 mm on the lathe, then cut to 42 mm length and mounted in the compound table for five 7 mm holes to be drilled perpendicular to the length through the rod at 8 mm from one end, then at 8 mm intervals through the length.

2.2.3 Gold Fragment Positioning Cup

A length of 8 mm nylon bar stock was turned down to 5.5 mm and a 4 mm hole drilled into its length to give a short tube.
The stock was parted after the end of the hole creating a short cup. From the same stock a small friction fitting cap for the cup was fabricated. The height of the cup with the lid attached was 5 mm.

2.2.4 Single Particle Instrument Response

A single fragment of ≥99.99% Au was immobilized on a small square of tape and inserted into the cup, which was capped and inserted into one of the holes in the positioning rod. The rod was then inserted into one of the holes in the positioning rig and the jar was capped and submitted to the PhotonAssay instrument for the PAAU02 service. The service was repeated 10 times and then the location of the particle was changed to determine the instrument response throughout the jar. The various locations are indicated in Table 1 and shown visually in Figure 4.

Table 1: Positions in the gold fragment positioning rig where PAAU02 tests were performed on a single fragment of gold.

Location	Distance from axis of rotation (mm)	Distance from jar bottom (mm)	Repeat analyses
1	0	7	5
2	0	21	5
3	0	35	5
4	14	7	5
5	14	21	5
6	14	35	5
7	28	7	5
8	28	21	5
9	28	35	5
10	32	7	5
11	32	21	5
12	32	35	5

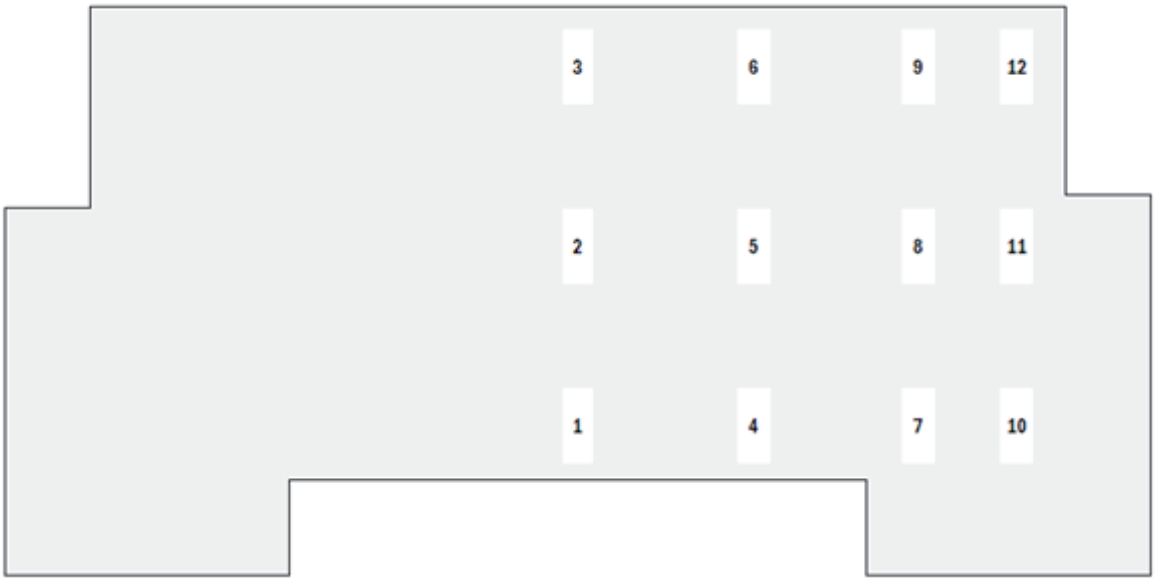

Figure 4: Schematic of the gold fragment positioning test rig in cross-section indicating the positions where a single fragment of gold was positioned and subjected to the PAAU02 service.

3. Results

3.1 Low-resolution Jar Map

The PhotonAssay-determined gold grades in the crushed rock jar (Table 2) show significant differences in the weighting of locations depending on both their distance from the axis of rotation and depth. The highest weighting is found in the geometric center of the jar (location 3). The repeat precision for locations along the axis of rotation (locations 1, 3 & 5) is consistent with precision at gold grades >1 ppm given by Chrysos Corporation [2]. However, repeat precision for gold fragment locations at the maximum distance from the axis of rotation (locations 2, 4 & 6) was significantly higher.

Results for the pulverized rock jar had a similar pattern of weighting, low repeat precision among repeat assays on the axis of rotation, and high precision among repeat assays far away from the axis of rotation (Table 3).

From the different weightings for the six locations, heat maps were constructed showing hotspots where fragments are strongly weighted, and cold spots where fragments receive weaker weighting (Figure 5).

Table 2: PhotonAssay results of the jar containing 100% passing 2 mm rock with a 1.011 mg gold fragment placed at locations 1 – 6 for 10 assays each. From the PhotonAssay-determined gold grade, the detected mass of gold, error against the weighed mass of gold, and the bias were calculated.

Location	n	Mean PA Au (ppm)	%RSD	Mean PA Au (mg)	Au Mass (mg)	Error (mg)	Bias
1	10	3.196	1.7%	1.236	1.011	0.225	+22%
2	10	1.959	4.5%	0.758	1.011	-0.253	-25%
3	10	4.673	1.4%	1.798	1.011	0.787	+78%
4	10	2.349	6.5%	0.908	1.011	-0.103	-10%
5	10	3.101	2.0%	1.199	1.011	0.188	+19%
6	10	1.417	2.7%	0.547	1.011	-0.464	-46%

Table 3: PhotonAssay results of the jar containing 85% passing 75 µm rock with a 1.051 mg gold fragment placed at locations 1 – 6 for 10 assays each. From the PhotonAssay-determined gold grade, the detected mass of gold, error against the weighed mass of gold, and the bias were calculated.

Location	n	Mean PA Au (ppm)	%RSD	Mean PA Au (mg)	Au Mass (mg)	Error (mg)	Bias
1	10	3.780	1.9%	1.147	1.051	0.096	+9%
2	10	2.292	5.2%	0.696	1.051	-0.355	-34%
3	10	5.962	1.8%	1.798	1.051	0.747	+71%
4	10	2.936	4.2%	0.889	1.051	-0.162	-15%
5	10	4.193	1.4%	1.268	1.051	0.217	+21%
6	10	1.954	2.7%	0.59	1.051	-0.461	-44%

Figure 5: Cross-sectional heat map depicting the relative weight given to regions of the jar in determining their gold grades by PhotonAssay. Due to the random rotational orientation of the jar during analysis, the is no differentiation between the sides of the heat map, and the diagram is symmetrical.

While both jars were completely filled with sample material, the instrument's fill-o-meter gave readings as low as 84.8% for the crushed material, and 94.0% for the pulverized material.

In every case, the average fill-o-meter reading across the 10 repeats was >96% for crushed material and >98% for pulverized material.

3.2 Medium-resolution Jar Map

The PhotonAssay-determined gold grades in the gold fragment positioning test (Table 4) show significant differences in the weighting of locations depending on both their distance from the axis of rotation and depth. As with previous tests, the highest weighting is found in the geometric center of the jar (location 2).

From the different weightings for the six locations, a heat map was constructed showing hotspots where fragments are strongly weighted, and cold spots where fragments receive weaker weighting (Figure 6).

Table 4: PhotonAssay results of the gold fragment positioning rig with a 0.504 mg gold fragment placed at locations 1 – 12 for 5 service runs each. From the PhotonAssay-determined gold grade, the detected mass of gold, error against the weighed mass of gold, and the bias were calculated.

Location	n	Mean PA Au (ppm)	%RSD	Mean PA Au (mg)	Au Mass (mg)	Error (mg)	Bias
1	5	2.364	0.83	0.702	0.504	0.198	+39%
2	5	2.706	1.47	0.804	0.504	0.300	+59%
3	5	1.745	2.40	0.518	0.504	0.014	+3%
4	5	2.258	5.23	0.671	0.504	0.167	+33%
5	5	2.6185	2.10	0.777	0.504	0.273	+54%
6	5	1.697	3.68	0.504	0.504	0.000	0%
7	5	1.690	2.89	0.502	0.504	-0.002	0%
8	5	2.179	4.24	0.647	0.504	0.143	+28%
9	5	1.494	0.70	0.444	0.504	-0.060	-12%
10	5	1.432	1.23	0.425	0.504	-0.079	-16%
11	5	1.668	2.38	0.495	0.504	-0.009	-2%
12	5	1.083	5.07	0.322	0.504	-0.072	-36%

Figure 6: Cross-sectional heat map depicting the relative weight given to specific locations of the jar in determining their gold grades by PhotonAssay. Due to the random rotational orientation of the jar about its axis of rotation during analysis, the is no differentiation between the sides of the heat map, and the diagram is symmetrical.

4. Discussion

Differences in the relative weighting of jar regions may originate during irradiation, measurement, a combination of both, or other factors not considered in this work.

4.1 Irradiation

For an excitation beam centered on the jar and narrower than the jar width, it is expected that gold fragments closer to the geometric center are more strongly activated, leading to higher weighting for that region, as was observed. Fragments far away from the axis of rotation are activated more strongly as they pass directly through the beam path, and less strongly at other times.

A fragment far from the axis of rotation will experience intermittent periods of excitation, the frequency of which is proportional to the rate of rotation. For rates of rotation where the period between excitation is large with respect to the half-life of 197mAu, differences in weighting may emerge. Fragments that end the irradiation cycle immediately before starting a period of excitation will have relatively low activity compared to those that end during or immediately after strong activation. This may be an explanation for the high repeat precision when far away from the axis of rotation observed in the low-resolution map experiments. Parameters of the process which to the knowledge of the authors are undisclosed would be required to evaluate further. It should be noted that in the medium-resolution map experiments, the higher RSDs at points further from the geometric center were not observed.
The activation of fragments at locations at the extreme top and bottom of the jar in the low-resolution experiments indicate that the beam width is at least equal to the height of the jar. The difference in weightings between low-resolution experiment locations 1 & 3 and locations 3 & 5 tends to suggest that the beam intensity across its width is higher at the center than the fringes. The difference in weighting between low-resolution experiment locations 1 & 5 tends to suggest that the beam intensity is higher at the bottom of the jar than the top. This was further indicated by the results of the medium-resolution experiments.

4.2 Measurement

The excitation beam's 8.5 MeV photons will be only minimally attenuated by the jar, the reference disc or the sample material. On the other hand, the 279 KeV gamma emissions from decaying 197mAu will experience significant attenuation for some paths ending at a detector. Additionally, some emission paths will not intersect a detector at all.

The degree of attenuation and the proportion of paths not intersecting a detector will be influenced by the activated fragment's position within the jar.

The most significant potential gamma attenuators are the reference disc and sample material itself. If gamma attenuation by the reference disc was the cause of differences in weighting for the jar regions, low-resolution experiment location 5 would be expected to have significantly less weighting than location 1. This is not observed, with positions 1 and 5 having similar weighting in the crushed rock jar, and position 5 having greater weighting in the pulverized rock jar. Similarly, we'd expect the medium-resolution map to show higher weighting for locations near the jar's boundaries, whereas the opposite was observed.

Gamma attenuation by the sample material would be highest for locations in the geometric center of the jar and lowest for locations at the top and bottom of the jar. In fact, the locations expected to experience greatest attenuation (low-resolution experiment location 3, and medium-resolution experiment location 2) had the highest weighting, making this unlikely to be the primary driver for the biases found.

Positions far from the axis of rotation would be expected to have a greater proportion of emission paths that do not intersect the detectors. This would result in lower weightings for low-resolution experiment locations 2, 4 & 6, which was observed. However, while locations 2 & 6 would experience this effect to similar degrees, location 4 would experience the greatest effect, giving even lower weighting. This is not observed, with location 4 having higher weighting than locations 2 & 6 for both jars.

Taken together, the results tend to indicate non-uniform irradiation during excitation as the more likely primary source of weighting differences observed between jar regions. If effects from gamma attenuation are present, they appear second-order, and obscured by the non-uniform irradiation.

4.3 Implications for Analysis

Understanding the different weighting assigned to regions within PhotonAssay jars has important implications for designing analytical protocols and interpretation of results.

A distinct advantage of true bulk analysis of 400 – 650 g samples is for the assaying of materials containing coarse gold fragments.

Coarse gold materials are challenging to sample due to high constitution heterogeneity arising from metallic gold's "nuggety" nature, and high distribution heterogeneity due to the tendency of dense gold particles to segregate [6]. Previous work by Minnitt, et al., using x-ray tomography to investigate behavior of gold fragments within simulated pulverized gold ore illustrated the tendency towards segregation in response to horizontal shaking [7].

PhotonAssay has demonstrated advantages over fire assay in accounting for higher levels of constitution heterogeneity when distribution heterogeneity is low [5]. However, unequal weighting of the jar's regions makes it vulnerable to grouping and segregation error, even after the final assay charge has been split from the lot. The PhotonAssay instrument's robotics transport jars, in part, by pushing them horizontally across surfaces. This motion may induce the type of segregation observed by Minnitt, et al. [7].

In as-of-yet-undisclosed results from a PhotonAssay user with which the authors are familiar, a large program of samples from an ore containing coarse gold were found to give a significant low bias for PA on <2mm crushed material vs fire assay. Understanding the low weighting assigned to fragments in the bottom and sides of the jar allows us to hypothesize that this bias originates from the segregation of coarse gold fragments.

5. Conclusions & Further Investigations

This work presents only low-to-medium resolution mapping of the weightings of jar regions. More comprehensive testing to include many increments of depth and between the center and edge of the jar would produce a fuller picture. A great deal more evaluation could be carried out with knowledge of parameters like the beam shape, width and consistency, as well as the rotation rate, precise geometry of the irradiation and measuring chambers, and the calculation of gold content from the HPGe signals. Further still, ability to control parameters such as rotation rate and rotational orientation would allow for better experimental design. Investigations of real-world coarse gold ore samples would further understanding of the interaction between comminution, segregation and PhotonAssay determinations. This could include size fraction analysis of ores known to display biases between PhotonAssay and fire assay, and possibly x-ray tomography of coarse gold ores within jars. Such work could ultimately be aimed at elucidating sample preparation and treatment protocols that account for and reduce the biases found in the present work.

ACKNOWLEDGEMENTS

The authors would like to thank Duncan Wright and Jonathan Lisk of Paragon Geochemical Laboratories for their kind assistance in preparing and assaying the gold-spiked materials used in this work.

References

[1] Z. Řanda, B. Špaček and J. Mizera, "Fast determination of gold in large mass samples of gold ores by photoexcitation reactions using 10 MeV bremsstrahlung," *Journal of Radioanalytical and Nuclear Chemistry*, vol. 271, no. 3, p. 603 – 606, 2006.

[2] Chrysos Corporation, "TN-003 PhotonAssay Measurement Performance for Precision Gold Services," 2024.

[3] Chrysos Corporation, "ChrysosPhoton Assay February 2024 Update,""" 2025. [Online]. Available: https://photonassay.com/. [Accessed 5 February 2025].

[4] C. H. Fulton, "*A Manual of Fire Assaying*," 2nd ed., New York, McGraw-Hill Book Company, 1911, p. 151.

[5] S. C. Dominy, J. C. Graham, K. H. Esbensen and S. Purevgerel, „Application of PhotonAssay™ to Coarse-Gold Mineralisation – the Importance of Rig to Assay Optimisation," *Sampling Science & Technology*, no. 1, p. 1 – 30, 2024.

[6] D. François-Bongarçon and M. Abzalov, "The Elusive Fine Gold Problem or the Distractive Power of Coarse Gold," in *The 11th World Conference of Sampling & Blending*, Johannesburg, 2024.

[7] R. C. A. Minnitt, S. C. Dominy and K. H. Esbensen, "Mixing is a Double-Edged Sword: the Grouping and Segregation Error on the Assayer's Bench," *Spectroscopy Europe*, vol. 34, no. 1, pp. 30-39, 2022.